


# An Augmented Airport Model for Ground Operations Analysis: A Case Study of Narita International Airport

Chelsea Shan Xian Ng[1], Michael Schultz[2] & Eri Itoh[1,3]

[1]Research Center for Advanced Science and Technology, The University of Tokyo
[2]Institute of Flight Systems, University of the Bundeswehr Munich
[3]Department of Aeronautics and Astronautics, The University of Tokyo

## Abstract

This work presents an augmented airport model that integrates a 3D-printed physical airport model with projected simulations of ground operations generated using a multi-agent simulator. The proposed framework aims to provide an intuitive means for visualizing and evaluating the effectiveness of airport operational strategies in reducing fuel consumption during taxiing. To demonstrate, single-engine taxi (SET) operations can be visualized through modified aircraft movement profiles and operational constraints governing feasible SET initiation regions. Aircraft ground trajectories can be rendered and projected onto the physical model to visualize surface movement, traffic interaction, as well as fuel consumed. Preliminary observations show the potential of the augmented airport model as a platform for visualizing and analyzing ground operations and communicating the impact of operational and infrastructural changes. The augmented airport model also features flexibility in its input and operation, establishing a foundation for future studies which potentially involve airport layout optimization and scheduling optimization strategies.

**Keywords:** airport ground operations, spatial visualization, augmented model, airport surface simulation, 3D printing,

## 1. Introduction

In response to the continuing growth of global air traffic, research in air traffic management has increasingly focused on improving operational efficiency across the different phases of flight, with particular emphasis on reducing fuel consumption and emissions. While the cruise and climb/descent phases have traditionally received significant attention, aircraft taxiing remains one of the least fuel-efficient phases of flight as aircraft engines do not operate within their optimum thrust range.[1] Prolonged taxiing, surface congestion and departure delays at complex aerodromes contribute to unnecessary fuel burn, making airport ground operations a critical area for intervention in pursuit of more sustainable aviation.[2], [3] The amount of emissions at an aerodrome can also be seen as a limiting factor in accommodating additional traffic. Reducing fuel burn during ground operations can potentially create operational headroom, allowing airports to handle more movement within the same environmental envelope. Beyond direct environmental benefits, improving fuel efficiency during taxiing will not only address the objective of sustainable aviation, but can also support growth of airport capacity by increasing its operational headroom.

A range of operational and infrastructural strategies have been proposed to reduce fuel consumption during taxiing.[4] These include alternative taxiing procedures such as single-engine taxi (SET), the use of dispatch towing vehicles, and broader optimization of airport surface operations through improved taxiway topology, routing, and scheduling.[5], [6] Single-engine taxi refers to when an aircraft taxis with half the number of its engines turned off, which is expected to reduce the overall fuel consumed during taxiing.[5] Previous work has demonstrated that the fuel-saving potential of SET is dependent on the combination of runway and spot, and the position where SET is initiated.[7]

https://doi.org/10.71945/icas2026_0272

This implies that SET cannot be applied uniformly across all ground operations (such as stipulating an initiation time of 1 minute after arrival across the board, for example), and its benefits can only be realized through consideration of airport layout and operational context.

The realization of efficiency enhancements through these operational and infrastructural strategies will involve multiple stakeholders such as airport operators, airlines, air traffic controllers, and ground handlers. Recent studies have highlighted the growing importance of integrated and data-driven platforms for improving airport operational awareness, visualization, and collaborative decision-making processes through approaches such as digital twins, and operational monitoring frameworks.[8], [9] However, spatially contextualized platforms that allow operational and infrastructural changes to be collectively visualized and evaluated by the various involved stakeholders remain relatively limited. Spatial cognition and shared situational understanding among stakeholders may play an important role in supporting collaborative decision-making. While conventional screen-based simulation outputs present operational data effectively from an analytical perspective, they may not always provide an intuitive understanding of how traffic interactions and congestion spatially evolved across the airport. As a result, the impact of proposed strategies on surface congestion, taxi times, and fuel consumption is not always communicated to the involved stakeholders in a clear and intuitive manner, limiting their practical adoption.

## 1.1 Narita International Airport

Narita International Airport (RJAA) is selected as a case study for this work due to its operational complexity and its role in supporting traffic demand for the Tokyo metropolitan area. Furthermore, planned redevelopment at RJAA aims to increase operational capacity while mitigating the associated impact on the environment.[10] RJAA currently has two parallel runways, Runway A (16R/34L) of length 4 km and Runway B (16L/34R) of length 2.5 km, and three separate passenger terminals. The planned changes include the construction of a new consolidated passenger terminal, a new cargo area, the extension of existing Runway B by 1 km, and the addition of a third parallel Runway C of 3.5 km. These redevelopments present an opportunity to revise ground operation procedures and taxiway configurations for eased congestion and increased efficiency in anticipation of rising traffic volumes. Currently, the extension of Runway B and the position and length of the new Runway C are confirmed changes. However, the positions and layouts of the associated taxiways, as well as those of the new passenger terminal and new cargo area, remain open for future redesign exploration and optimization. An illustration of the planned changes is provided in Figure 1.

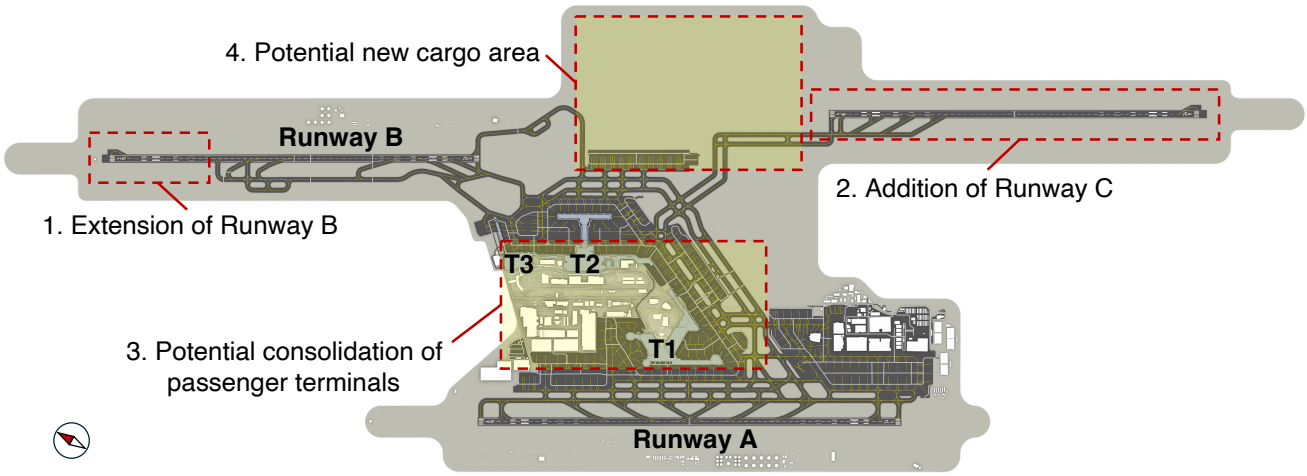



Figure 1 – The planned changes for Narita International Airport (RJAA). The extension of Runway B and new Runway C are confirmed, while the consolidated passenger terminal and new cargo area are yet to be confirmed. The names of terminals 1, 2, and 3 are abbreviated to T1, T2, and T3, respectively.

To support these planned modifications, the physical airport model is designed to be modular with swappable components for passenger terminals, aprons, taxiways, and runways. This modularity allows alternative layout scenarios to be physically reconfigured and compared, facilitating exploration of both current and proposed aerodrome configurations.

## 2. Proposed Methodology

In this work, an augmented airport model is proposed as a platform for analyzing and communicating ground operation optimization strategies. The proposed approach integrates a scaled, 3D-printed model of an airport with simulation data dynamically projected onto the model surface allowing aircraft ground movements and operational metrics to be visualized directly on a tangible representation of the airport. The combination of the physical model of the airport with the projected results of simulated ground movement together creates our augmented airport model. An overview of the augmented airport model is shown in Figure 2.

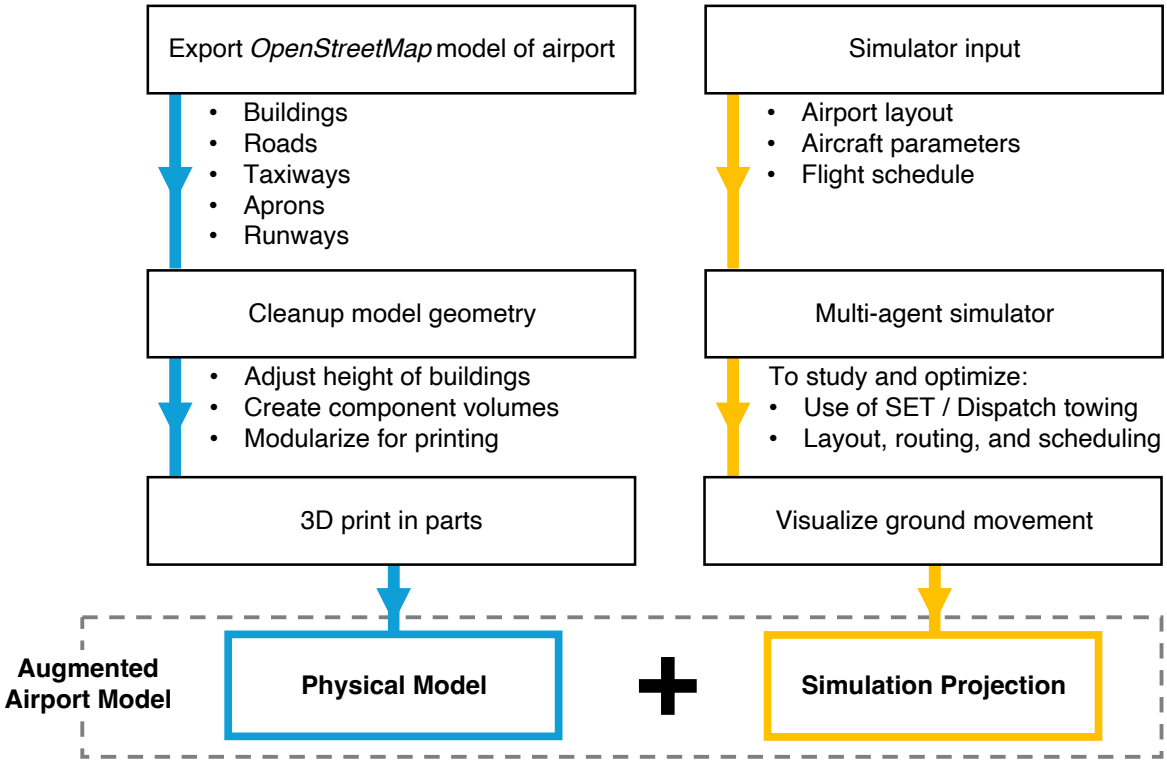



Figure 2 – An overview of the augmented airport model which comprises of a 3D-printed physical model and projections from a multi-agent simulator.

Unlike traditional static airport models which are primarily illustrative platforms, or purely virtual simulations viewed on monitor screens, the proposed augmented model aims to provide stakeholders with an enhanced spatial understanding of the implications of alternative ground operation strategies and infrastructural modifications, supporting evaluation and facilitating informed discussions.

### 2.1 Physical model fabrication

A virtual model of Narita International Airport (RJAA) is created via data obtained from *OpenStreetMap* (OSM), exported using *Overpass Turbo*. The exported data includes the footprints of buildings in and around the airport, as well as roads, taxiways, and runways as polylines. The model was imported into and edited in *Rhinoceros* to include the planned extension for Runway B and the new Runway C. The positions of the current terminal buildings and cargo areas remain unchanged. Simple taxiways are added to connect the new Runway C to the rest of the taxiway network, referencing images published by Narita Airport.[10] The positions of the spots from the

OSM data agree well with their published coordinates in the Aeronautical Information Publication (AIP) of RJAA, and so they remain unchanged. The height of the buildings and other geometric details for the control and ramp towers are approximated and modelled after images from *Google Maps*. The polylines representing roads, taxiways, and runways were converted into surfaces with widths of 8 m, 30 m, and 60 m, respectively.

This virtual model was scaled down by a factor of 5000 for 3D printing in an Original Prusa XL 5-toolhead printer. The model was separated into different components; a base plate, terminal buildings, aprons, taxiways, and runways. Suitable thicknesses for printing were created for the aprons, taxiways, runways, and also the base plate. Specifically, the base plate has a thickness of 1.4 cm, the aprons, taxiways, and runways have thicknesses of 0.6 cm, (each layer of the print has a thickness of 0.2 cm). Additionally, the markings on aprons, taxiways, and runways were also given a thickness Each of the components are also modularized due to the printer's limited volume of 36 cm x 36 cm x 36 cm. The base plate is designed to have slots, and the aprons, taxiways, and runways have corresponding protrusions under them to help position them on the base plate. Separating the model into different components is done to facilitate later reconfigurations of the airport layout. In this way, new taxiway configurations can be printed to replace the current designs when needed. To illustrate, Figure 3A shows the 3D-printed model of the original configuration of the airport, with swappable components placed on the sides. In Figure 3B, the extension for Runway B, the new Runway C, and the associated taxiways are swapped in and added to the airport model. Creating the model to have swappable parts in this manner will allow us to print future redesigns and swap them in on-demand. For the base plate, each modularized part took an approximate average of 3 hours to be printed, and for the taxiways and buildings, each modularized part took an approximate average of 1 hour to be printed. The primary material used for printing was PLA (polylactic acid), and because the printer used was a multi-tool printer, we could easily print the different components with different colors at the same time. As such, we could print the taxiways and their markings with colors that matched their real-world appearance.

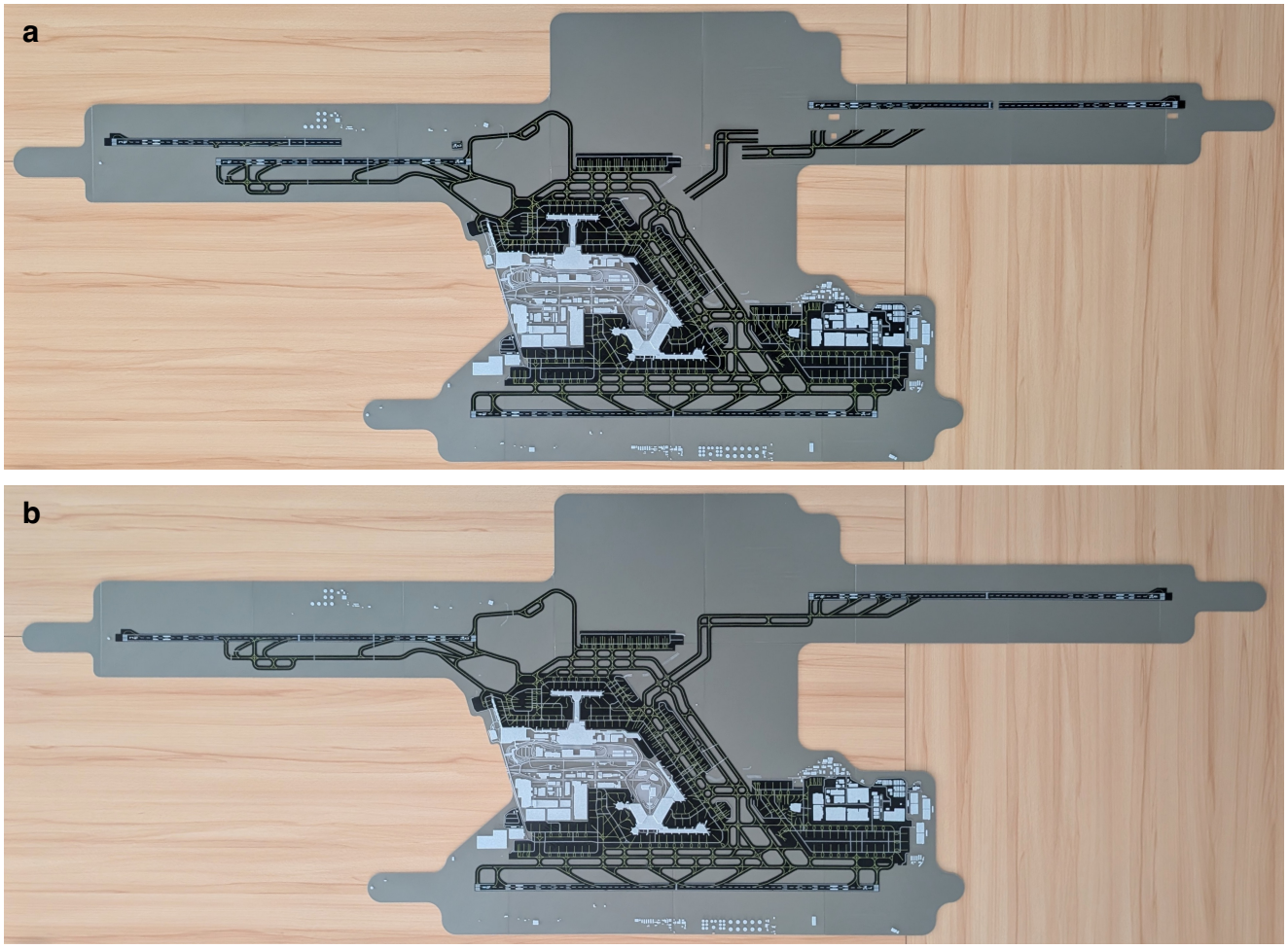



Figure 3 – 3D-printed Narita Airport Model with a scale of 1:5000 in its a) original, current configuration, and its b) new configuration. The new configuration shows the extension of Runway B and addition of Runway C through swapping components in.

## 2.2 Multi-agent simulator (MAS)

A multi-agent simulator (MAS) was developed to create simulations of ground movement at RJAA. [11] The MAS is coded in python and receives input through an excel workbook containing information on the layout of the airport, schedule, departure and arrival routes, aircraft parameters such as velocity and fuel consumption rate, and other parameters related to surface management. This input also includes the total simulation time, and duration of each time step of the simulation in seconds. The outputs of the simulation are the positions of aircraft (or agent) in each user-specified timestep for the given duration, as well as their total fuel consumed. These results can then be rendered and visualized using *ParaView* before being projected onto the physical model.

From the airport model which uses polylines with straight segments to represent taxiways and runways in *Rhinoceros*, we can derive data for the nodes and edges of the taxiway graph using a *Grasshopper* script. Nodes, which correspond to spots, intersections, and turning points, are represented with point entities. Through modifying the point properties in *Rhinoceros*, the nodes are named alphanumerically according to their respective spot name or taxiway name with a prefix based on where they are found. Nodes found on the runway, taxiway, apron, and spot are labelled with the prefixes R-, T-, A- and S-, respectively. The node positions are specified in their cartesian coordinates in meters, with the airport reference point (ARP) set as the origin. The *Grasshopper* script extracts these node names and coordinates into a csv file which is in turn read by the MAS python code.

The edges of the taxiway graph are specified using their origin node and their destination node, as the edge direction, length, and position in the cartesian space can be found through the coordinates

of these nodes. The edge information is used to create four directed graphs which correspond to combinations of north or south wind conditions, with arrival or departure routes. The route taken for a particular agent will be the shortest path in the corresponding directed graph connecting the node where the agent enters the simulation to the node where it exits. For instance, in north wind conditions, an agent with an entry node having the prefix R- (indicating that it is an arriving aircraft) would take the shortest path connecting this entry node and its exit spot node that can be found in the directed graph for arrivals under north wind conditions. Conversely, given south wind conditions, an agent with an entry node having the prefix S- (indicating that it is a departing aircraft) will take the shortest path connecting its entry and exit runway node found in the directed graph for departures under south wind conditions. Note that only nodes with R- and S- can be specified for the entry and exit nodes. For each of these four directed graphs, the *Grasshopper* script extracts the names of the origin and destination nodes of its respective edges into four csv files.

The layout of the airport can be modified within *Rhinoceros*, and new node and edge input data can be regenerated with the same *Grasshopper* script. This implies that future renditions of the airport layout can be easily implemented through this pipeline. In the same vein, the layouts of other airports can be loaded into the MAS to simulate their ground movement.

Aside from the layout of the airport, the MAS also requires the schedule of the agents which is a list of the agent names, entry times, entry and exit nodes, prevailing wind and aircraft type. Table 1 summarizes the details of the input schedule.

Table 1 – Schedule details to input into the multi-agent simulator.

| Parameter | Description |
|---|---|
| **Name** | Labelled starting from 1 according to the chronological entry time. It can also be changed to the agent's callsign. |
| **Entry time** | The time at which the agent enters the simulation, in hours. |
| **Entry node** | The name of the node at which the agent enters the simulation. |
| **Exit node** | The name of the node at which the agent exits the simulation. |
| **Wind** | The prevailing wind direction during the agent's existence within the simulation, i.e., north or south. |
| **Aircraft type** | The type of aircraft of the agent, i.e., light, medium, heavy, super. |

The MAS also accepts an input of movement profiles, that specify the agent's taxi speeds, $v$, and fuel consumption rates, $f$. These parameters differ along different phases of its route, such as runway, taxiway, and apron movement, and holding for traffic. The agents will assume an appropriate movement profile based on its aircraft type and its position in the route, ultimately allowing us to calculate their overall temporal positions, and fuel consumed through the simulation. Through these movement profiles, we can also simulate when the aircraft uses single-engine taxi (SET) by adding on new sets of values for $v$, and $f$. Table 2 gives an example of these movement profiles which we use in later simulations. In Table 2, $v$ and $f$ are given in $ms^{-1}$ and $kgs^{-1}$, respectively. Due to lack of data currently, we assign simplified representative velocity and fuel flow rate values for each aircraft type and movement profile. These parameters are intended to support preliminary comparative simulation of ground movement at the current stage rather than provide high-fidelity aircraft performance modelling. Since specific aircraft types are expected to have varying $v$ and $f$, more rows can be appended to Table 2 to assign corresponding average values for the different states of specific aircraft types if they are known.

Table 2 – Movement profiles for different aircraft types.

| Aircraft Type | | Runway | Runway Exit | Stop-Start | Stop-Start SET | Taxiway High | Taxiway | Taxiway SET | Apron | Apron SET |
|---|---|---|---|---|---|---|---|---|---|---|
| Light | $v$ / ms$^{-1}$ | 40 | 11.0 | 0.0 | 0.0 | 9.0 | 7.0 | 7.0 | 3.0 | 3.0 |
| | $f$ / kgs$^{-1}$ | 0.9 | 0.26 | 0.12 | 0.18 | 0.24 | 0.20 | 0.10 | 0.16 | 0.08 |
| Medium | $v$ / ms$^{-1}$ | 50 | 10.0 | 0.0 | 0.0 | 8.5 | 6.5 | 6.5 | 2.8 | 2.8 |
| | $f$ / kgs$^{-1}$ | 1.8 | 0.52 | 0.24 | 0.34 | 0.46 | 0.40 | 0.20 | 0.30 | 0.15 |
| Heavy | $v$ / ms$^{-1}$ | 55 | 9.0 | 0.0 | 0.0 | 8.0 | 6.0 | 6.0 | 2.5 | 2.5 |
| | $f$ / kgs$^{-1}$ | 3.2 | 0.95 | 0.42 | 0.58 | 0.85 | 0.75 | 0.38 | 0.55 | 0.28 |
| Super | $v$ / ms$^{-1}$ | 60 | 8.0 | 0.0 | 0.0 | 7.5 | 5.5 | 5.5 | 2.2 | 2.2 |
| | $f$ / kgs$^{-1}$ | 5.0 | 1.55 | 0.70 | 0.95 | 1.35 | 1.20 | 0.60 | 0.90 | 0.45 |

Note that in reality, aircraft accelerate and decelerate during the take-off and landing phases, respectively. However, the current implementation does not yet distinguish between take-off and landing movement profiles within the runway segments of the taxiway network. In addition, here the movement along the runway uses a simplified representation using equivalent constant velocity values instead of acceleration profiles. The assigned $v$ and $f$ values for the runway movement profile are selected to approximate the representative runway occupancy behavior for each aircraft type. This preliminary simplified representation may be further refined in future work through the incorporation of more detailed runway operation modelling.

The simulation runs through each time step with each agent's position calculated and updated based on its assigned route, velocity, and interaction with other agents. On the runways, a duration is specified to prevent other agents from entering the runway; this is known as the runway separation time which differs depending on the aircraft type and the type of the preceding aircraft due to wake turbulence. The runway separation time also depends on whether the aircraft are departure or arrival aircraft. Based on this we can form a matrix for runway separation time shown in Table 3, where the duration is listed in seconds.

Table 3 – A matrix of runway separation times for each pair of types of aircraft, listed in seconds.

| | | | Current Aircraft | | | | | | | |
|---|---|---|---|---|---|---|---|---|---|---|
| | | | Arriving | | | | Departing | | | |
| | | | Light | Medium | Heavy | Super | Light | Medium | Heavy | Super |
| Preceding Aircraft | Arriving | Light | 100 | 100 | 100 | 100 | 75 | 75 | 75 | 75 |
| | | Medium | 105 | 105 | 100 | 100 | 80 | 75 | 75 | 75 |
| | | Heavy | 120 | 120 | 105 | 105 | 80 | 80 | 75 | 75 |
| | | Super | 120 | 120 | 120 | 120 | 80 | 80 | 80 | 80 |
| | Departing | Light | 75 | 75 | 75 | 75 | 85 | 85 | 85 | 85 |
| | | Medium | 80 | 80 | 75 | 75 | 90 | 90 | 85 | 85 |
| | | Heavy | 95 | 95 | 85 | 85 | 105 | 105 | 90 | 90 |
| | | Super | 95 | 95 | 95 | 95 | 105 | 105 | 105 | 105 |

The runway separation times shown in Table 3 are calculated based on the 10$^{th}$ percentile of observed runway separation times over 28 days of operational data, rounded to the nearest integer. We obtained this data from CARATS Open Data (Collaborative Actions for Renovation of Air Traffic Systems) for the first seven days of the months September to December in 2019.

To simulate interaction on the taxiways and aprons, a collision radius is specified in the input which is used to determine when any two agents are in conflict with one another. Agents at the spot nodes are excluded from the following conflict resolution logic. The Euclidean distance between each pair of agents is calculated; if the separation distance falls below the collision radius threshold, they are considered to be in potential conflict, and a decision must be made for one of either aircraft to stop movement. The type of interaction and their respective actions can be classified into the following (Table 4, simplified from [12]):

Table 4 – The types of interactions and their respective actions to be taken.

| Type | Interaction | Action |
|---|---|---|
| A | Both agents are on the same edge and are travelling in the same direction. | The trailing agent is stopped while the leading agent can continue moving. |
| B | Both agents are on different edges travelling towards the same node. | If a stop command for one of the agents exists in a previous step, it is kept and the other agent is allowed to continue moving. If not, agents exiting a runway are given priority over taxiing aircraft. Arriving aircraft are also given priority over departing aircraft. Else, one of the agents is selected at random to stop. |

For type A interactions where both agents are on the same edge and travelling in the same direction, the trailing agent is stopped while the leading agent continues its motion. Note that this logic results in a sequential following behavior that maintains aircraft separation while allowing traffic to continue flowing, similar to queue formation in high traffic conditions. For type B interaction where both agents are on different edges and travelling towards the same node, the agent which received a stop command in a previous time step will preserve its state and the other agent is allowed to continue its motion. If neither agent has received a stop command in the previous time step, the agent which is exiting a runway is given priority, that is, it is allowed to continue its motion while the other agent is stopped. Likewise, arriving aircraft are given priority over departing aircraft. However, if the aircraft are both arriving or both departing, one is selected at random to stop while the other continues its motion.

Because the directed graphs representing the routes for aircraft on arrival or departure rarely possess overlapping edges of opposing directions, it is unlikely that head-on interactions on the same edge will occur. However, if they do occur, arriving aircraft are given priority over departing aircraft. If no priority exists, one aircraft is randomly selected to stop.

## 2.3 Integration and visualization

The proposed augmented airport model integrates the physical model with the MAS through a projection-based visualization workflow. The objective of this integration is to provide an intuitive, spatial representation of aircraft ground movement which can facilitate the study of operational strategies and their effectiveness in reducing fuel consumption during taxiing. We believe that by combining the physical model of the airport with simulation outputs, the augmented model serves as a platform to observe traffic interactions in a more immersive manner compared to conventional screen-based visualization methods.

The output of the MAS, consisting of the temporal positional data of each aircraft agent, can be visualized and rendered in *ParaView*. In the current implementation, the aircraft are represented as moving point objects that travel along the airport taxiway network. A top-down rendering is generated as a video sequence, showing the movement of aircraft over time. This rendered visualization allows aircraft movement patterns, queue formation, and traffic interactions to all be seen at a glance. While this preliminary visualization uses simplified point representations, future extensions can use more detailed aircraft geometries and also show additional operational indicators for the agent.

To align the rendered visualization of the MAS output with the physical airport model, the projected image is scaled according to the dimensions of the physical model. The projector is positioned directly above the physical model to give a top-down projection. The lateral position of the projection and the physical model can be calibrated using reference anchor points positioned at known locations on both the rendered video and the physical model. Such calibration is important to maintain the spatial consistency between the virtual simulation and the physical model, particularly when visualizing aircraft movement across complex taxiway intersections and at terminal areas.

In this work, we focus on showing the implementation of SET as an initial demonstration of how operational optimization strategies can be visualized within the augmented airport model (see Section 3.2). To support SET operations, the movement profiles to the multi-agent simulator are updated to incorporate modified fuel flow rates associated with SET procedures, together with the SET initiation points along each taxi route. This enables the simulation to account for the operational differences between conventional taxi and SET, to finally allow us to compare the fuel consumed

and saved.

In addition to aircraft movement visualization, the augmented airport model is intended to also support the visualization of congestion and traffic interactions within the taxiway network. Areas where agents come within their collision radius or experience movement conflicts can be highlighted within the rendered projection. Once the congestion is resolved, the highlighted regions can be removed accordingly. Although this functionality has not been fully implemented in the current study, the proposed visualization approach demonstrates how traffic bottlenecks and operational inefficiencies can be indicated. Such visual indicators can potentially support future studies into taxiway topology optimization, terminal layout modifications, and scheduling optimization targeted at improving the efficiency of ground operations and reducing fuel consumption.

## 3. Implementation and Results

Here the setup of the augmented airport model was completed with the 3D-printed model of Narita International Airport (RJAA) and its projected simulations from the multi-agent simulator (MAS). To demonstrate the visualization of ground operations using the augmented airport model, we simulate the use of single-engine taxi (SET) at RJAA and its effectiveness in saving fuel.

### 3.1 Setup

The physical model is assembled on a table measuring 2.65 m by 1.40 m (the physical model itself measures 2.46 m by 0.88 m when fully assembled with the extension of Runway B and new Runway C). The physical model is oriented to have the airport runways parallel to the longer edge of the table to provide a more intuitive viewing perspective of aircraft movement. This arrangement also gives good visibility of aircraft trajectories and congestion areas during observation of the simulation. A custom support frame was constructed to position the projection system directly above the physical model. The projector is fixed 1.5 m above the table to achieve our top-down projection of the rendered simulation. Although projectors capable of direct downward projection are commercially available, the projector used in the current implementation had limitations in its mounting orientation. To overcome this constraint, an angled mirror was incorporated into the setup to redirect the projected image vertically downward onto the table surface. Figure 4 illustrates the overall setup of the augmented airport model.

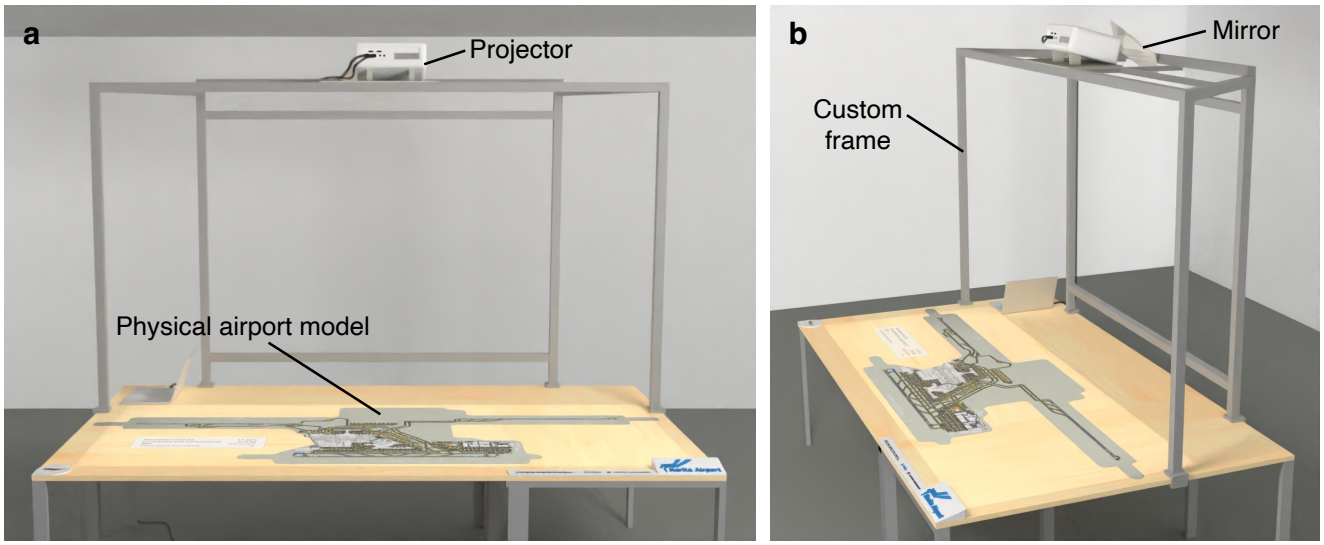



Figure 4 – An illustration of the setup of the augmented airport model. a) The front view showing the projector positioned directly above the physical airport model. b) A perspective view showing the custom frame to hold the projector and a mirror to direct the projection down.

The relative lateral position of the physical model and projector are manually calibrated by moving the physical model. The scale and orientation of the projection is manually adjusted from the

projector settings, while tuning the relative lateral position is achieved through moving the physical model. Calibration is performed by matching reference points, which can be prominent taxiway intersections, runway thresholds and terminal positions.

## 3.2 Demonstrating the visualization of SET operations

To demonstrate the application of the augmented airport model, the current study focuses on the visualization and preliminary implementation of SET operations. Through this approach, the differences between conventional taxi operations and SET operations can be visualized directly on the physical airport model. The implementation of SET operations within the MAS is achieved by modifying the aircraft movement profiles used during simulation. The movement profiles define the operational behavior of the aircraft under different surface movement conditions, including taxiing on normal taxiways, aprons, runways, or high-speed taxiways, and stop or idle conditions. The movement profile parameters currently adopted in the simulation framework are summarized in Table 2, including the velocity and fuel flow values, for each operational state under both conventional taxi and SET. These profiles form the basis for simulating and estimating fuel consumption during airport surface operations.

The simulation schedule used is based on airport operational data obtained from CARATS Open Data for September 14$^{th}$ in 2019 at RJAA. This date was chosen from the data we currently have access to due to its higher traffic volume, clear weather, and absence of flights that go around. Since the extension of Runway B and the new Runway C are still only planned additions, they are excluded from the simulation input; the current layout of RJAA is used in the simulation. The resulting airport layout rendered from the MAS, including a sample of the aircraft positions at 17.40 h is illustrated in Figure 5.

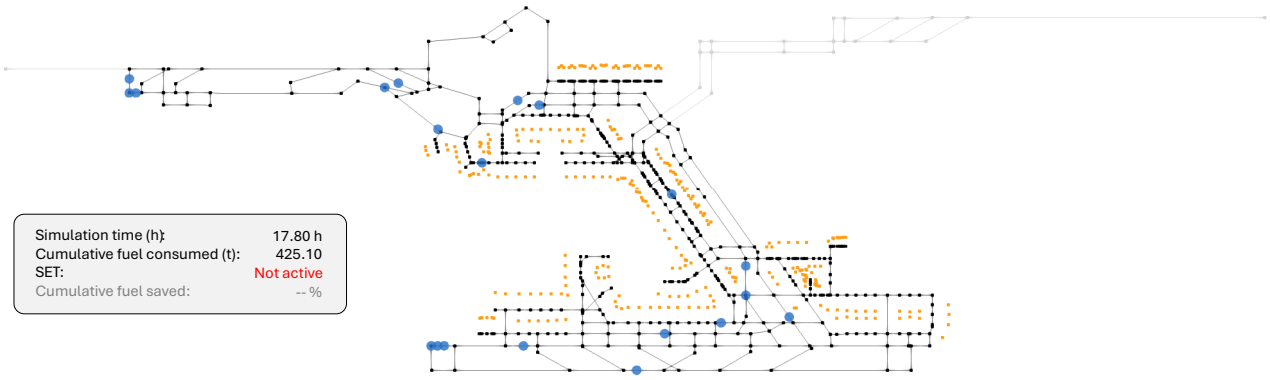



Figure 5 – The simulation output rendered with *ParaView*, showing a top-down view of the taxiway network at Narita International Airport (RJAA) along with the simulation time, cumulative fuel consumed, single-engine taxi (SET) utilization status, and cumulative fuel saved. The taxiways are represented with black lines, the spots are represented as yellow dots, and the agents are represented with a blue circle. The lines representing the extension of Runway B and new Runway C are greyed out as were not utilized in this simulation. In this snapshot, a queue formation can be observed at the entrance to Runway A (16R).

The visualization framework also supports the representation of fuel consumption metrics. Fuel consumption estimates are calculated for both baseline operations without SET and operations incorporating SET procedures. Rather than presenting absolute fuel consumption values, a relative percentage of fuel savings achieved through SET implementation is shown instead. This normalizes the results across different aircraft types with varying baseline fuel consumption rates and will allow more consistent comparisons of operational improvements. Here, we assume that all aircraft initiate SET at their respective earliest feasible position along their assigned taxi routes. As the simulation time progresses, the projected visualization can display a continuously updated cumulative fuel savings value of using SET relative to baseline operations. This allows the operational performance

to be observed temporally throughout the simulation period to give a more intuitive representation of the effectiveness of SET procedures on fuel saving.

To determine the earliest feasible position to initiate SET, we look at the assigned taxi routes for each combination of runway and spot. We assume that the assigned taxi route is the shortest distance between the runway and spot in the respective taxiway network (see Section 2.2). The ranges along each route where SET initiation is valid are determined by a set of geometric and operational constraints:[13]

1. A minimum engine cooldown time must elapse after exiting the runway, $t_{\mathrm{cool}}$
2. A certain distance away from the runway, $d_{\mathrm{rwy}}$
3. A certain distance before reaching the spot, $d_{\mathrm{spot}}$
4. SET can only be initiated once and remains active until the aircraft reaches the spot
5. Not a certain distance before a turn, $d_{\mathrm{turn}}$
6. Not on an upslope section, $\theta_{\mathrm{slope}}$

For our simulations, $t_{\mathrm{cool}}$, $d_{\mathrm{rwy}}$, $d_{\mathrm{spot}}$, and $d_{\mathrm{turn}}$, are set at 180 s, 200 m, 100 m, and 50 m, respectively. While these constraints are assigned with representative values for this preliminary study, if more accurate values are known, they can be modified as required in the input to the MAS. Figure 6 illustrates the implementation of these constraints for selected arrival routes. Figures 6a-c show arrival routes for Runways A, B, and C, in north wind conditions towards Spot 21, and in south wind conditions towards Spot 402L. Note that because arrivals at Runway C are only planned for north wind conditions, only one route is shown in Figure 6c. The selected spots in this figure were chosen primarily to demonstrate routes located closer to different runways within the airport layout. In Figure 6, red-highlighted regions indicate sections of the taxi route where SET initiation is infeasible due to constraint violations, while green-highlighted regions represent where SET initiation is feasible. To satisfy the fourth constraint, we consider the two parallel high-speed taxiways located at the south side of the taxiway network (shown in Figure 6b). Conventional full-engine taxi may be more suitable along such segments due to the higher taxi speeds involved. SET initiation is therefore limited to only after the aircraft has passed these sections of its taxi route, avoiding the need for engine restart procedures which may introduce additional fuel penalties and reduce the effectiveness of SET operations. In our current simulations, the point along each route where the first green segment is encountered is selected as the SET initiation point for that agent or aircraft.

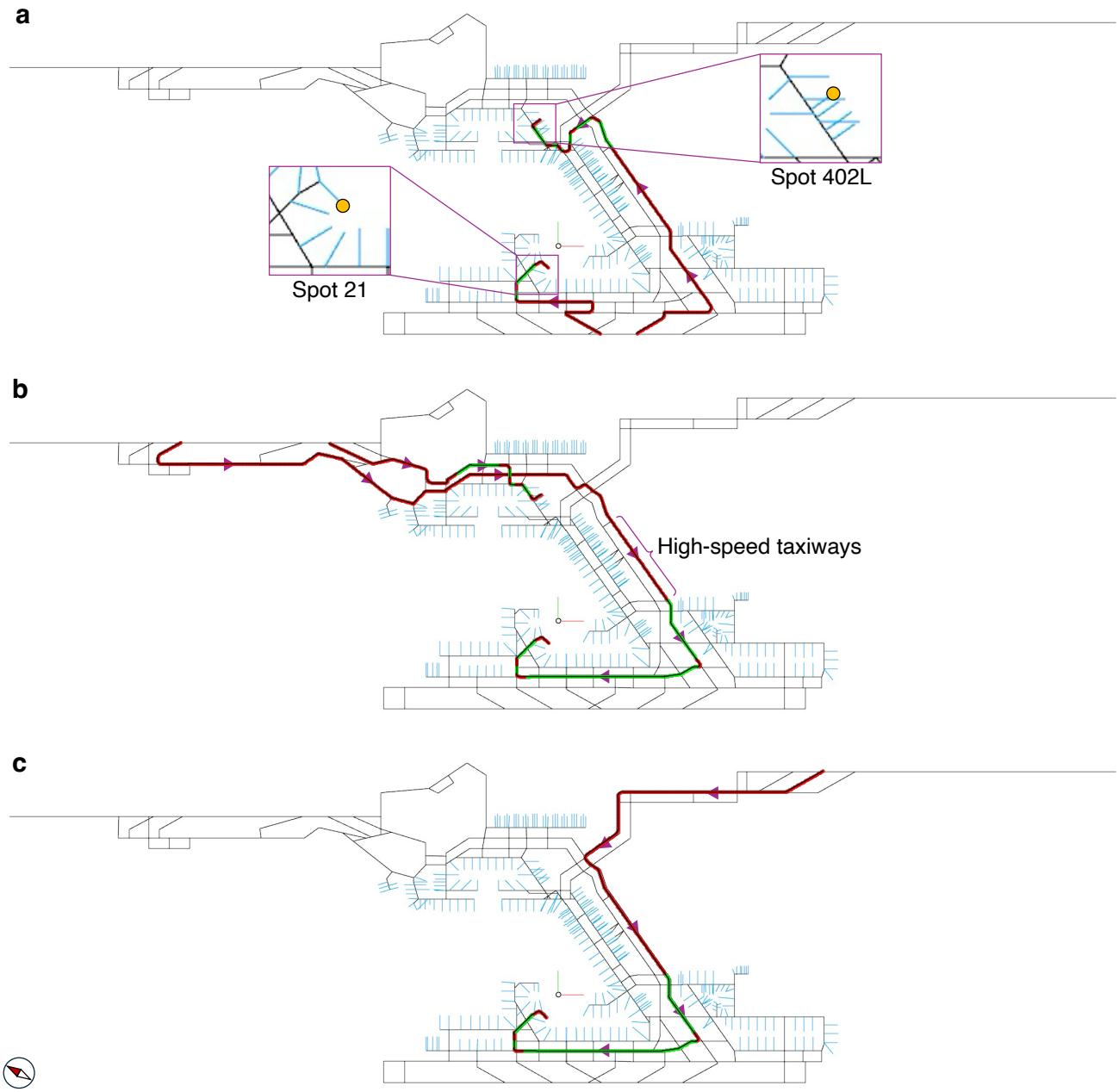



Figure 6 – The range of single-engine taxi (SET) initiation points considering the geometric and operational constraints for a) Runway A, b) Runway B, and c) Runway C. For each subfigure, the routes are shown from runway to Spot 21 for north wind conditions, and from runway to Spot S-402L for south wind conditions. Note that arrivals are currently planned for Runway C only during north wind conditions, hence one route is shown accordingly. Red-highlighted regions indicate where SET initiation is infeasible while green-highlighted regions represent where SET initiation is feasible. The purple arrows indicate the direction of travel.

At the current stage, the constraints remain partially implemented in the simulation. While taxiway turns are considered in the routes to determine the feasible SET initiation regions, they are not included in the simulation yet and will be in future iterations of the MAS. Our current virtual airport model also assumes a flat surface due to the unavailability of detailed airport elevation and slope data. Hence, the upslope constraint is presently inactive within the simulation. However, the simulation framework is structure such that elevation information can be incorporated directly into the taxiway network input through the assignment of three-dimensional node coordinates ($x$, $y$, and $z$), where the $z$ coordinate corresponds to the local surface elevation. Future implementations of the MAS can hence account for the slope constraint with minimal modification to the existing simulation framework.

### 3.3 Preliminary analysis and observations

The goal of the augmented airport model is to allow the analysis of airport surface operations through the combined use of the multi-agent simulator and the projection of its output onto a tangible, physical model. Although the simulation framework is still under development at present, it demonstrates how operational modifications such as SET procedures and its effectiveness can be visualized and compared within the augmented model environment. The framework serves as an initial platform for investigating airport operational strategies through numerical outputs and spatial visualization.

Currently, the augmented airport model demonstrates the capability to support both quantitative and qualitative analysis of airport surface operations. While we have focused primarily on the visualization of SET procedures and estimated fuel savings, additional operational metrics can potentially be incorporated. These may include taxi duration, reduction in taxi times, waiting times, congestion frequency. Emissions estimation may also be possible, if emission rates are known, by refining movement profiles to include such operational parameters.

Apart from being able to generate tabulated numerical summaries from the simulation output, the augmented model provides a means of presenting operational information directly together with the physical model. Fuel savings and congestion hotspots can be visualized dynamically on the airport model throughout the simulation period. Compared to conventional simulation outputs that are limited to the screen, the augmented model may provide a more intuitive spatial understanding of airport traffic and operations. Embedding the simulation output directly within the physical airport model provides spatial contextualization, potentially enabling shared situational and spatial awareness among multiple users or stakeholders and facilitating more collaborative evaluation of operational and infrastructural modifications. Understanding the spatial implications of proposed changes in this manner will be beneficial for future studies involving operational strategies and the optimization and redesign of the airport layout.

Preliminary observations from the current simulation outputs suggest that aircraft interactions occur frequently at gateways where aircraft merge paths when entering or exiting the apron area. As expected, queue formation can be observed near runway entry points where aircraft accumulate prior to departure. Observing these phenomena through the augmented airport model can provide a more intuitive understanding of traffic movement and localized congestion behavior. Such observations demonstrate the potential of the augmented model for identifying regions within the taxiway network that may require infrastructural improvement, which may be beneficial for future studies involving taxiway layout optimization and airport surface planning.

The modular structure of the physical airport model further supports such future developments as individual components can be modified, reprinted, and replaced where necessary. This capability is demonstrated is evident through being able to swap out the components to represent the runway extension, as well as the addition of the new runway and its associated taxiways. Corresponding updates to the airport layout can be subsequently incorporated into the MAS to generate updated outputs and visualizations. This flexibility allows the augmented model to not only function as a visualization platform, but also an experimental testbed for studying alternative airport configurations.

## 4. Discussion and Future Work

The augmented airport model at this stage represents an initial framework for integrating airport surface simulation with projection-based visualization on a physical airport model. To facilitate its development, several simplifying assumptions were adopted at the current stage. As a result, there remain several key limitations with the current implementation which provide opportunities for future development and refinement.

Currently, aircraft movement within the multi-agent simulator (MAS) is represented using simplified movement physics and taxiway geometry. The taxiway network is modelled using straight polyline segments connected at nodes, resulting in sharp, abrupt turns. The dynamic behavior of aircraft during turning maneuvers are also not fully incorporated into the movement simulation. In practice, taxiways are curved at the nodes and aircraft have to reduce their taxi speed when executing turns.

This will result in reduced taxi distance and also altered movement profiles compared to their current simplified movement. While taxiway turns have been considered geometrically during determination of feasible single-engine taxi (SET) initiation regions, it has not yet been represented within the simulator. Future work will hence extend the simulator and movement profiles to simulate more realistic turning behavior, including speed reduction and curved taxi trajectories.

Currently, SET optimization within the MAS is based on the geometric and operational constraints associated with the layout of the airport. The agents initiate SET at the earliest feasible position along their taxi routes once all predefined constraints are satisfied. While the feasible SET initiation segments vary according to the runway and spot combination,[7] the current framework has yet to account for the influence of prevailing traffic conditions on the effectiveness of SET operations. Under realistic operating conditions, surface congestion may impact the optimal SET initiation point as aircraft may have to stop-and-go repeatedly due to traffic. This may introduce additional fuel penalties that could reduce or negate the expected fuel savings associated with initiating SET as early as possible; we hypothesize that the earliest feasible SET initiation point may not necessarily correspond to the optimal SET initiation point under realistic traffic conditions. Future work will extend the current framework by simulating traffic conditions in order to deduce the optimal SET initiation point.

Another current limitation is the absence of validation against real-world operational data. Although the MAS is capable of generating aircraft movement trajectories and operational metrics, the simulation accuracy remains to be quantitatively compared to real airport surface operations. Future work will therefore focus on validating the simulator outputs against real-world scenarios, including comparisons of taxi duration, queue formation behavior, and importantly, the fuel consumed and saved. Doing so will solidify the predictive capability and realism of the augmented airport model.

Future developments can also extend the current pre-rendered projections towards real-time, interactive visualization. This can potentially be achieved through the use of a game engine such as *Unity*, which could streamline the input method while enabling dynamic rendering of simulation outputs. Transforming into such an approach would allow interactive observation of ground movement at the airport with varying traffic conditions and optimization strategies. Since future developments include changes to the airport layout, it will be beneficial to be able to change the layout of the physical model while being able to update the simulation output on demand. Within this interactive environment also, agents or aircraft could be selected to display their individual operation status such as taxi information and estimated fuel savings.

Increased user interaction may also boost the augmented airport model. At present, interaction with the augmented airport model remains primarily observational, where stakeholders (the users) can view the projected simulation outputs on the physical airport model. Future iterations of the augmented airport model may explore how users can actively participate in evaluating airport operational strategies and layout modifications. This could include the use of interactive controls for scenario manipulation, for example. Another aspect which can be enhanced is the immersion of using the augmented airport model, to which virtual and augmented reality technologies may provide a solution. User studies or focus group evaluations may be required to assess the usability and interpretability of the augmented visualization framework for different stakeholders. Such pilot studies would provide insight into the practical value of the augmented airport model in real-world decision-making and communication, particularly for future operational and infrastructural modifications to the airport.

In future, extending the augmented airport model towards a digital twin framework may also be beneficial. Currently, the flow of information is unidirectional, where inputs from the real-world system are fed into the MAS, and its outputs are projected onto the physical airport model for visualization and analysis. In contrast, a digital twin environment would involve a continuous exchange of information between the virtual and physical systems in real time.[8], [14] Such an approach also increases user interaction, and the augmented airport model may therefore evolve beyond a mere visualization platform into a more interactive environment for supporting airport operational planning

and management.

Finally, the proposed methodology can potentially be extended to other airports beyond the current case study. Positional data of the airport layout will be required for 3D printing (or other suitable fabrication methods). Having this information along with the desired schedule to be studied, the ground movement at the airport can be simulated accordingly using the MAS. The parameters of the MAS can also be customized accordingly to adapt to desired scenarios, especially in terms of the movement profiles. Perhaps, the simulation can also include not just aircraft for agents but also ground vehicles that share the same airside space. This indicates the potential scalability of the augmented airport model as a general platform for studying and visualizing airport ground operations.

## 5. Conclusion

In summary, this work proposes an augmented airport model for the purpose of examining and communicating the potential of ground operation optimization strategies. While the initial showcase of this work shows the implementation of single-engine taxi operations to reduce fuel flow, the augmented model is projected to also serve as a platform for studying the broader range of airport ground operation optimization problems, such as taxiway topology design, routing, and scheduling. Moving beyond conventional screen-based simulation platforms, the proposed approach provides a tangible, spatial environment where simulation results can be explored and communicated, potentially supporting collaborative decision-making in airport ground operations aimed at reducing emissions and accommodating future traffic growth.

## 6. Acknowledgements

This study was supported by research funding provided by Japan Airlines Co., Ltd and the JAL Aviofuture Lab. The authors also gratefully acknowledge Professor Yoshiaki Kawagoe of Tohoku University for his invaluable support and contributions to the preliminary development of the multi-agent simulator environment.

## 7. Contact Author Email Address

Correspondence concerning this work should be addressed to the corresponding author at eriitoh@g.ecc.u-tokyo.ac.jp.

## 8. Copyright Statement

The authors confirm that they, and/or their company or organization, hold copyright on all of the original material included in this paper. The authors also confirm that they have obtained permission, from the copyright holder of any third party material included in this paper, to publish it as part of their paper. The authors confirm that they give permission, or have obtained permission from the copyright holder of this paper, for the publication and distribution of this paper as part of the ICAS proceedings or as individual off-prints from the proceedings.

## 9. References

[1] Khadilkar, H. and H. Balakrishnan. Estimation of Aircraft Taxi-out Fuel Burn using Flight Data Recorder Archives, in *AIAA Guidance, Navigation, and Control Conference*, Portland, Oregon: American Institute of Aeronautics and Astronautics, Aug. 2011.

[2] Avogadro, N. and R. Redondi. Pathways toward sustainable aviation: Analyzing emissions from air operations in Europe to support policy initiatives, *Transp. Res. Part Policy Pract.*, Vol. 186, p. 104121, 2024.

[3] Dzikus, N., J. Fuchte, A. Lau, and V. Gollnick. Potential for Fuel Reduction through Electric Taxiing, in *11th AIAA Aviation Technology, Integration, and Operations (ATIO) Conference*, Virginia Beach, VA: American Institute of Aeronautics and Astronautics, Sep. 2011.

[4] Dahanayaka, M., D. Prak, and M. Mes. From gate to runway: A systematic review of airport ground operations optimization, *J. Air Transp. Manag.*, Vol. 135, p. 103013, 2026.

[5] Guo, R., Y. Zhang, and Q. Wang. Comparison of emerging ground propulsion systems for electrified aircraft taxi operations, *Transp. Res. Part C Emerg. Technol.*, Vol. 44, pp. 98–109, 2014.

[6] Lukic, M., P. Giangrande, A. Hebala, S. Nuzzo, and M. Galea. Review, Challenges, and Future Developments of Electric Taxiing Systems, *IEEE Trans. Transp. Electrification*, Vol. 5, No. 4, pp. 1441–1457, 2019.

[7] Funaba, R., K. Matsuo, K. Tominaga, and E. Itoh. Estimation of fuel consumption reduction by the SET operations at Narita Int'l Airport, in *SESAR Innovation Days 2024*, Rome, 2024, p. 2024070.

[8] Conde, J., A. Munoz-Arcentales, M. Romero, *et al.* Applying digital twins for the management of information in turnaround event operations in commercial airports, *Adv. Eng. Inform.*, Vol. 54, p. 101723, 2022.

[9] Schultz, M., J. Rosenow, and X. Olive. Data-driven airport management enabled by operational milestones derived from ADS-B messages, *J. Air Transp. Manag.*, Vol. 99, p. 102164, 2022.

[10] Capacity Enhancement of Narita Airport. Accessed: Sep. 09, 2025. [Online]. Available: https://www.narita-kinoukyouka.jp/en/

[11] Kawagoe, Y., R. Chino, S. Tsuzuki, E. Itoh, and T. Okabe. Analyzing Stochastic Features in Airport Surface Traffic Flow Using Cellular Automaton: Tokyo International Airport, *IEEE Access*, Vol. 10, pp. 95344–95355, 2022.

[12] Tsuzuki, S., D. Yanagisawa, and K. Nishinari. Throughput reduction on an air-ground transport system by the simultaneous effect of multiple traveling routes equipped with parking sites, *J. Phys. Commun.*, Vol. 4, No. 5, p. 055009, 2020.

[13] Koudis, G. S., S. J. Hu, A. Majumdar, W. Y. Ochieng, and M. E. J. Stettler. The impact of single engine taxiing on aircraft fuel consumption and pollutant emissions, *Aeronaut. J.*, Vol. 122, No. 1258, pp. 1967–1984, 2018.

[14] Tao, F., H. Zhang, A. Liu, and A. Y. C. Nee. Digital Twin in Industry: State-of-the-Art, *IEEE Trans. Ind. Inform.*, Vol. 15, No. 4, pp. 2405–2415, 2019.